Chaos, Solitons and Fractals 168 (2023) 113167

Contents lists available at ScienceDirect

Chaos, Solitons and Fractals

journal homepage: www.elsevier.com/locate/chaos

Determining Lyapunov exponents of fractional-order systems: A general method based on memory principle

Hang Li [a], Yongjun Shen [b,c], Yanjun Han [c], Jinlu Dong [a], Jian Li [a,*]

[a] Key Laboratory of Structural Dynamics of Liaoning Province, College of Science, Northeastern University, Shenyang 110819, China
[b] State Key Laboratory of Mechanical Behavior and System Safety of Traffic Engineering Structures, Shijiazhuang Tiedao University, Shijiazhuang 050043, China
[c] Department of Mechanical Engineering, Shijiazhuang Tiedao University, Shijiazhuang 050043, China

ARTICLE INFO

Keywords:
Lyapunov exponent
Fractional-order systems
Memory principle
Chaos

ABSTRACT

Lyapunov exponents provide quantitative evidence for determining the stability and classifying the limit set of dynamical systems. There are several well-established techniques to compute Lyapunov exponent of integer-order systems, however, these techniques failed to generalize to fractional-order systems due to the nonlocality of fractional-order derivatives. In this paper, a method for determining the Lyapunov exponent spectrum of fractional-order systems is proposed. The proposed method is rigorously derived based on the memory principle of Grünwald–Letnikov derivative so that it is generally applicable and even well compatible with integer-order systems. Three classical examples, which are the fractional-order Lorenz system, fractional-order Duffing oscillator, and 4-dimensional fractional-order Chen system, are respectively employed to demonstrate the effectiveness of the proposed method for incommensurate, nonautonomous and low effective order systems as well as hyperchaotic systems. The simulation results suggest that the proposed method is indeed superior to the existing methods in accuracy and correctness.

1. Introduction

Lyapunov exponent (LE) was introduced by Oseledets [1] in his multiplicative ergodic theorem. Based on Oseledets's theory, Benettin et al. [2] first reported the method of calculating all LEs of dynamical systems. Later, Wolf et al. [3] improved Benettin's method, and first proposed the method of estimating LEs from time series based on Takens's reconstruction technique [4], the latter one is widely used in experimental research. In addition to the Benettin-Wolf algorithm, various works on the calculation scheme of LE have been reported in the last four decades, mainly including determination from governing equations [5,6] and estimation from time series [7,8]. Moreover, researchers have developed perturbation methods, such as the perturbation vectors approach [9] and the cloned dynamics approach [10], as well as the synchronization method [11]. Such methods avoid directly calculating the Jacobian matrix or solving the variational equations so that they can be applied to more cases, for example, the non-smooth system, which generally has an ill-conditioned Jacobian matrix. At present, the above methods have been effectively applied to dynamical characterization in several fields [12–15]. Fractional calculus (FC) is an ancient branch of calculus theory. In the early stage, unlike classical calculus, FC had more research in pure mathematical theory, but sporadic applications in physics (summarized by Valério, et al. [16]). In the past two decades, many more researchers have paid attention to the interdisciplinary applications of FC since some problems can be elegantly modeled by FC in a novel way, such as the mechanical behavior of viscoelastic materials [17–19], the image encryption [20,21], and the epidemic modeling [22,23]. Recently, Diethelm, et al. [24] and Sun, et al. [25] reviewed the application of FC in physics and engineering, respectively.

Generally, the solutions of fractional-order differential equations cannot define a dynamical system in the sense of semigroup [26], however, it does not mean that the relationship between fractional-order differential equations and their phase flows cannot be established in a similar way to integer-order ones. As a measure of the convergence or divergence rate of phase flows, LE is still a powerful mathematical tool for studying the dynamic evolution of fractional-order systems (FOS). Li et al. [27] introduced a rigorous mathematical definition of LE of FOS for the first time and proposed a method to determine its bounds. In addition, some new methods, such as time series methods [28,29] and the extended Benettin-Wolf algorithm [30], have been developed to estimate LEs of FOS. In these advances, it is confirmed that LE is still valid for determining stability, fractal dimension and limit set. However, there are some limitations, for instance, extended Benettin-Wolf algorithm is more suitable for quasi-integer-order systems due

* Corresponding author.
E-mail address: jianli@mail.neu.edu.cn (J. Li).

https://doi.org/10.1016/j.chaos.2023.113167
Received 15 October 2022; Received in revised form 20 December 2022; Accepted 18 January 2023
Available online 24 January 2023

to the fact that the nonlocality is insignificant enough to be ignored. In fact, the nonlocality of FOS implies that the convergence and/or divergence of phase flow is history-dependent, thus well-established methods in integer-order systems are difficult to be generalized in FOS. Therefore, by formulizing the history-dependent relationship of the convergence (or divergence) in all dimensions, all LEs of FOS can be determined correctly, which is the main contribution of this work.

2. The proposed method

2.1. Preliminaries

The basic idea of the proposed method is as follows. By discretizing the continuous-time system based on the numerical method of fractional differential equations (FDEs), deviations in entire time–history, which is caused by a small initial perturbation, is also formulized as a discrete mapping. It is well known that LE is defined by the mean logarithmic growth rates of deviation, thus it can be easily calculated from the deviation. The LE spectrum is determined by perturbing each dimension of the system, in which Gram–Schmidt orthonormalization procedure is used to solve the numerical divergence problem caused by the positive LE.

Consider an n-dimensional (n-D) continuous-time system described by

$$D_t^{\boldsymbol{q}}\boldsymbol{x}(t) = \boldsymbol{f}(\boldsymbol{x}) \tag{1}$$

where $\boldsymbol{x} = (x_1, x_2, \dots, x_n)^{\mathrm{T}} \in \mathbb{R}^n$, and $\boldsymbol{f}(\boldsymbol{x}) = (\boldsymbol{f}_1(\boldsymbol{x}), \boldsymbol{f}_2(\boldsymbol{x}), \dots, \boldsymbol{f}_n(\boldsymbol{x}))^{\mathrm{T}}$ is a real-valued n-D vector function. $D_t^{\boldsymbol{q}}\boldsymbol{x} = (D_t^{q_1}x_1, D_t^{q_2}x_2, \dots, D_t^{q_n}x_n)^{\mathrm{T}}$, in which $D_t^{q_i}$ is the fractional-order derivative operator $\frac{\mathrm{d}^{q_i}}{\mathrm{d}t^{q_i}}$ (for $0 < q_i < 1$) or the integer-order derivative operator $\frac{\mathrm{d}}{\mathrm{d}t}$ (for $q_i = 1$), $i = 1, 2, \dots, n$.

For the integer-order case, the deviation between two phase trajectories caused by an initial perturbation $\boldsymbol{w}(t_0)$ is generally governed by

$$\dot{\boldsymbol{w}} = \boldsymbol{J}_f\boldsymbol{w}, \tag{2a}$$

$$\boldsymbol{w}(t_0) = \boldsymbol{x}(t_0) - \overline{\boldsymbol{x}}(t_0) \tag{2b}$$

where $\boldsymbol{J}_f = \mathrm{d}\boldsymbol{f}/\mathrm{d}\boldsymbol{x}$ is the Jacobian matrix of $\boldsymbol{f}(\boldsymbol{x})$.

LE is generally defined by the mean logarithmic growth rates of the deviation, i.e.,

$$\lambda = \lim_{t\to\infty}\frac{1}{t}\ln\frac{\|\boldsymbol{w}(t)\|}{\|\boldsymbol{w}(t_0)\|} \tag{3}$$

Some of the methods just mentioned, such as the symplectic method [5] and singular value decomposition method [6], also involve solving Eqs. (2). In fact, Eqs. (2) describes the long-term growth of the n-D ellipsoid size defined by the deviation $\boldsymbol{w}$, and the growth rate obeys LE. Note, that for the fractional-order case, LE is still defined by Eq. (3), but the deviation should not be described by Eqs. (2) due to the nonlocality of the FOS. To the best of the authors' knowledge, there are few unified schemes to describe the nonlocality of deviation $\boldsymbol{w}$. The following will solve the problem and introduce a general method to determine all LEs of FOS.

2.2. Procedures

The next work focuses on the fractional-order case of Eqs. (1). There are three widely used definitions of fractional-order derivative, namely Grünwald–Letnikov (G–L) definition, Riemann–Liouville definition and Caputo definition, and more details about their characteristics, differences and relations can be learned in the Refs. [31,32].

Particularly, the numerical scheme of Eqs. (1) can be derived by applying the memory principle of G–L definition. Here, the scheme is regarded as an n-D mapping, and it is governed by

$$\boldsymbol{x}(t_{k+1}) = \boldsymbol{F}(\boldsymbol{x}(t_k), t_k) \tag{4}$$

where $t_k = kh$, and h is the integration time-step. $\boldsymbol{F} = (\boldsymbol{F}_1, \boldsymbol{F}_2, \dots, \boldsymbol{F}_n)^{\mathrm{T}}$, and $\boldsymbol{F}_i$ is given by

$$\boldsymbol{F}_i(\boldsymbol{x}(t_k), t_k) = \boldsymbol{f}_i(\boldsymbol{x}(t_k))h^{q_i} - \sum_{r=1}^{k+1} C_r^{(q_i)}x_i(t_{k+1-r}) \tag{5}$$

where $C_r^{(q_i)}$ is the fractional binomial coefficient [33] obeying $C_0^{(q_i)} = 1$, $C_r^{(q_i)} = (1 - (1 + q_i)/r)C_{r-1}^{(q_i)}$.

The evolution of the deviation between two mappings caused by an initial perturbation $\boldsymbol{w}^{(0)}$ is governed by

$$\begin{aligned}\boldsymbol{w}^{(k+1)} &= \boldsymbol{J}_F^{(k)}\boldsymbol{w}^{(k)} = \boldsymbol{J}_F^{(k)}\boldsymbol{J}_F^{(k-1)}\boldsymbol{w}^{(k-1)} = \cdots = \prod_{s=0}^{k}\boldsymbol{J}_F^{(s)}\boldsymbol{w}^{(0)}\\ &= \boldsymbol{A}^{(k)}\boldsymbol{w}^{(0)} = \sum_{i,j=1}^{n} w_i^{(0)}\boldsymbol{a}_j^{(k)}\end{aligned} \tag{6}$$

where $w_i^{(0)}$ and $\boldsymbol{a}_j^{(k)}$ are, respectively, the i-th element of $\boldsymbol{w}^{(0)}$ and the j-th column of $\boldsymbol{A}^{(k)}$, and $\boldsymbol{J}_F^{(k)} = \mathrm{d}\boldsymbol{F}/\mathrm{d}\boldsymbol{x}|_{t=t_k}$, but $\boldsymbol{J}_F^{(k)}$ cannot be directly obtained from Eqs. (4). Fortunately, if $\lim_{k\to\infty}\boldsymbol{J}_F^{(k)}$ exists, the general iterative scheme of $\boldsymbol{A}^{(k)}$ can be obtained from the tangent map of Eq. (5), in which the element $a_{i,j}^{(k)}$ obeys the following mapping.

$$a_{i,j}^{(k+1)} = h^{q_i}\frac{\partial \boldsymbol{f}_i}{\partial x_j}a_{i,j}^{(k)} - \sum_{r=1}^{k+1} C_r^{(q_i)}a_{i,j}^{(k+1-r)} \tag{7}$$

The initial value $\boldsymbol{A}^{(0)}$ should be set to the identity matrix $\boldsymbol{I}$.

To calculate all LEs of Eqs. (4), n sets of initial perturbation $\boldsymbol{W}^{(0)} = (\boldsymbol{w}_1^{(0)}, \boldsymbol{w}_2^{(0)}, \dots, \boldsymbol{w}_n^{(0)}) = \mathrm{diag}(\varepsilon_1, \varepsilon_2, \dots, \varepsilon_n)$ are taken to perturb each dimension of the system, where $\varepsilon_i \neq 0$. According to Eq. (6), the deviation matrix is given by

$$\boldsymbol{W}^{(k+1)} = \boldsymbol{A}^{(k)}\boldsymbol{W}^{(0)} \tag{8}$$

Thus, it can be derived from Eqs. (3) and (6) that the j-th LE of Eqs. (4) satisfies the following relationship.

$$\begin{aligned}\lambda_j &= \lim_{t_k\to\infty}\frac{1}{t_k}\ln\frac{\|\boldsymbol{w}_j^{(k+1)}\|}{\|\boldsymbol{w}_j^{(0)}\|} = \lim_{k\to\infty}\frac{1}{kh}\ln\frac{|\varepsilon_j|\|\boldsymbol{a}_j^{(k)}\|}{\|\boldsymbol{w}_j^{(0)}\|}\\ &= \lim_{k\to\infty}\frac{1}{kh}\ln\|\boldsymbol{a}_j^{(k)}\|\end{aligned} \tag{9}$$

Generally, $\lambda_1 \geq \lambda_2 \cdots \geq \lambda_n$, otherwise, they are rearranged.

Note that when $k \to \infty$, all columns of $\boldsymbol{A}^{(k)}$ tend to line up with $\boldsymbol{a}_1^{(k)}$ so that all calculated LEs would be close to λ_1. In addition, $\lambda_1 > 0$ implies that $\boldsymbol{A}^{(k)}$ is unbounded, which would lead to numerical divergence problem. For more details, one can refer to the perturbation subspace discussed in Ref. [34].

Inspired by Wolf et al. [3], Gram–Schmidt orthonormalization procedure is also used to solve the above two problems in the iteration of Eq. (7). Let the orthonormalization time-step be $h_{\mathrm{norm}} = Nh$, and then perform the following orthonormalization procedure at $k = N, 2N, \dots, KN$, where $N \in \mathbb{N}$.

$$\begin{aligned}\boldsymbol{v}_1^{(k)} &= \boldsymbol{a}_1^{(k)}\\ \boldsymbol{a}_1^{(k)} &= \frac{\boldsymbol{v}_1^{(k)}}{\|\boldsymbol{v}_1^{(k)}\|}\\ \boldsymbol{v}_2^{(k)} &= \boldsymbol{a}_2^{(k)} - \left\langle \boldsymbol{a}_2^{(k)}, \boldsymbol{a}_1^{(k)}\right\rangle\boldsymbol{a}_1^{(k)}\\ \boldsymbol{a}_2^{(k)} &= \frac{\boldsymbol{v}_2^{(k)}}{\|\boldsymbol{v}_2^{(k)}\|}\\ &\vdots\\ \boldsymbol{v}_n^{(k)} &= \boldsymbol{a}_n^{(k)} - \left\langle \boldsymbol{a}_n^{(k)}, \boldsymbol{a}_1^{(k)}\right\rangle\boldsymbol{a}_1^{(k)} - \cdots - \left\langle \boldsymbol{a}_n^{(k)}, \boldsymbol{a}_{n-1}^{(k)}\right\rangle\boldsymbol{a}_{n-1}^{(k)}\\ \boldsymbol{a}_n^{(k)} &= \frac{\boldsymbol{v}_n^{(k)}}{\|\boldsymbol{v}_n^{(k)}\|}\end{aligned} \tag{10}$$

Finally, the j-th LE of Eqs. (1) can be calculated in the following way.

$$\lambda_j = \lim_{K\to\infty} \frac{1}{K h_{\text{norm}}} \sum_{\kappa=1}^{K} \ln \|\boldsymbol{v}_j^{(\kappa N)}\| \tag{11}$$

where K indicates that the orthonormalization procedure has been repeated K times. Empirically, h_{norm} can be selected in a wide range due to the calculated result is not sensitive to that. In this paper, it is taken as $h_{\text{norm}} = 10h$, unless otherwise specified.

2.3. Discussions on the proposed method

(1) One can understand the proposed method in the following way. Recalling Eq. (6), $\boldsymbol{J}_F^{(k)}$ can be regarded as the linear transformation from $\boldsymbol{w}^{(k)}$ to $\boldsymbol{w}^{(k+1)}$. $\boldsymbol{A}^{(k)}$ is the accumulation of k-times linear transformation, i.e., the linear transformation directly from $\boldsymbol{w}^{(0)}$ to $\boldsymbol{w}^{(k+1)}$. Furthermore, $\boldsymbol{A}^{(k)}$ is obtained from tangent map of Eqs. (4), in which the orthogonalization procedure ensures that the n sets of deviation are independently measured to obtain all LEs, and ensures that the measurement benchmark is reset K times to avoid the numerical divergence problems.

(2) It can be found that when $q_i = 1$, Eqs. (4) degenerate to the forward Euler scheme, i.e., $\boldsymbol{x}(t_{k+1}) = \boldsymbol{x}(t_k) + h\boldsymbol{f}(\boldsymbol{x}(t_k))$, so that $\boldsymbol{J}_F^{(k)}$ in the integer-order case can be directly obtained by $\boldsymbol{J}_F^{(k+1)} = \boldsymbol{I} + h\boldsymbol{J}_f^{(k)}$. Based on this, it can be derived from Eq. (6) that $\boldsymbol{A}^{(k+1)} = (\boldsymbol{I}+h\boldsymbol{J}_f^{(k)})\boldsymbol{A}^{(k)}$, which is precisely the degenerate version of Eq. (7) at $q_i = 1$, or in other words, the tangent map of the forward Euler scheme. Therefore, the first discussion is still valid, and the proposed method can be directly applied to integer-order systems.

(3) Phase trajectory divergence is a characteristic of chaotic systems, and it is measured by LE. This means that the calculated result of LE depends on the system itself rather than the numerical method. In addition, despite relying on G–L method, the proposed method is based on the rigorous derivation and does not require manual tuning. Thus, Eq. (9) can be regarded as an approximation scheme of the exact value of LE. Based on these, it can be inferred that another discretization method would produce an approximation scheme with higher or lower accuracy, which would not lead to a fundamental difference in results. Therefore, using a higher-order discretization method to improve accuracy can be considered as a direction for future research.

3. Numerical verification

3.1. Incommensurate case

The first example demonstrated is the fractional-order Lorenz system [33], and it is governed by

$$D_t^{q_1} x_1 = \sigma(x_2 - x_1) \tag{12a}$$

$$D_t^{q_2} x_2 = Rx_1 - x_2 - x_1 x_3 \tag{12b}$$

$$D_t^{q_3} x_3 = x_1 x_2 - Bx_3 \tag{12c}$$

In this case, the simulation conditions are taken as $\boldsymbol{x}(0) = (20, 10, 50)^{\mathrm{T}}$, $h = 0.0005$, $t_{\text{final}} = 100$, and three sets of order Q_1: $(q_1, q_2, q_3) = (0.985, 0.99, 0.98)$, Q_2: $(q_1, q_2, q_3) = (0.985, 0.97, 0.98)$, and Q_3: $(q_1, q_2, q_3) = (1, 1, 1)$ are tested. Lorenz system is considered as a model of thermal convection, in which σ is called the Prandtl number, and in which R is called the Rayleigh number. Here, they are set to $\sigma = 16$, $R = 45.92$, and $B = 4$, since such parameters lead to an well accepted LE values in the integer-order case, which will be discussed later.

For the Q_1 set, the chaotic attractor shown in Fig. 1(a) can be obtained, and the corresponding LEs determined by the proposed method are 1.0586, −0.0933, and −25.3930, respectively. The time histories of LEs and x_1 are shown in Fig. 1(b) and 1(c), respectively. It can be found from Fig. 1(c) that the response of Eqs. (12) is quasi-periodic before $t = 33$, and then the response develops into chaos, which exactly consistent with the increase of λ_1 at $t = 33$ in Fig. 1(b).

For the Q_2 set, the limit set of Eqs. (12) is the asymptotically stable equilibrium point as shown in Fig. 2, and the corresponding three negative LEs are −0.1391, −0.1581, and −24.9487. It is easy to obtain that the three equilibrium points of Eqs. (12) are $E_1(0, 0, 0)$, $E_2(-\sqrt{B(R-1)}, -\sqrt{B(R-1)}, R-1)$, and $E_3(\sqrt{B(R-1)}, \sqrt{B(R-1)}, R-1)$. Here, the trajectory is attracted to E_3 due to the initial values $\boldsymbol{x}(0)$ close to E_3. In addition, it is worth noting that if $h_{\text{norm}} = 5h$ in the Q_2 set, the corresponding three LEs are −0.1333, −0.1566 and −24.9753, and if $h_{\text{norm}} = 25h$, the three LEs are −0.1560, −0.1626 and −24.8447. In short, h_{norm} can be selected in a wide range, which will not lead to large fluctuation in results.

For the Q_3 set, the standard integer-order case, the well accepted reference values [7] of LEs are 1.5, 0, and −22.5, and the corresponding values calculated by the proposed method are 1.5143, 0.0617, and −22.6085, respectively. This result shows that the proposed method is indeed compatible with integer-order systems.

3.2. Low effective order and hyperchaotic case

The second example is to demonstrate the validity of the proposed method for hyperchaotic systems as well as for systems with low effective order (i.e., the sum of all orders). In four (or more) dimensional systems such as the 4-D fractional-order Lorenz systems [35,36], Rössler systems [35,37] and Chen systems [36,38,39], there may be hyperchaotic attractors, which exhibit two (or more) positive LEs. The difference with the other two systems lies in the fact that chaotic attractors can be generated by the 4-D fractional-order Chen systems at a lower effective order. Therefore, to simultaneously verify that the proposed method is valid for systems with low effective order, the following 4-D fractional-order Chen system [38] is demonstrated here as the second example.

$$D_t^{\alpha} x_1 = 36(x_2 - x_1) \tag{13a}$$

$$D_t^{\alpha} x_2 = -16x_1 - x_1 x_3 + 28x_2 - x_4 \tag{13b}$$

$$D_t^{\alpha} x_3 = x_1 x_2 - 3x_3 \tag{13c}$$

$$D_t^{\alpha} x_4 = x_1 + 0.5 \tag{13d}$$

In this case, three orders, $\alpha = 0.95$, $\alpha = 0.88$ and $\alpha = 0.78$, are tested. The initial condition is always set as $\boldsymbol{x}(0) = (0, 0, 8, 6)^{\mathrm{T}}$ and the time step is fixed as $h = 0.001$. Moreover, 40 time units are simulated at $\alpha = 0.95$ and $\alpha = 0.88$, 200 time units are simulated at $\alpha = 0.78$, and then the three corresponding simulation results are as shown in Figs. 3, 4 and 5, respectively. The correspondences [40] between the signs of LEs and the limit set of 4-D systems are listed in Table 1 for reference.

The existence of hyperchaotic attractors in 4-D fractional-order Chen-family systems has been validated in several existing studies [36, 38,39]. Similarly, here the 4-D Chen system (13) at $\alpha = 0.95$ generates a chaotic attractor as shown in Fig. 3(a) and 3(b), and the corresponding LEs determined by the proposed method are 1.2534, 0.2788, −0.0018 and −21.6758, as shown in Fig. 3(c). Therefore, the attractor is also hyperchaotic.

As aforementioned, chaotic attractors can be generated by the 4-D Chen systems at a lower effective order. As shown in Fig. 4(b), it is obtained by the proposed method that the LEs of system (13) at $\alpha = 0.88$ are 1.5246, 0.0813, −0.6944 and −39.1704, respectively, and the corresponding limit set is indeed a chaotic attractor as shown in Fig. 4(a). In addition, the simulation results of the system at $\alpha = 0.78$ shows periodic motion as shown in Fig. 5(a), and the corresponding LEs obtained by the proposed method are −0.0066, −0.9901, −5.2612 and −86.1648, as shown in Fig. 5(b).

In summary, the above results agree well with the correspondence listed in Table 1, thus it is validated that the proposed method is effective for hyperchaotic systems as well as systems with low effective order.

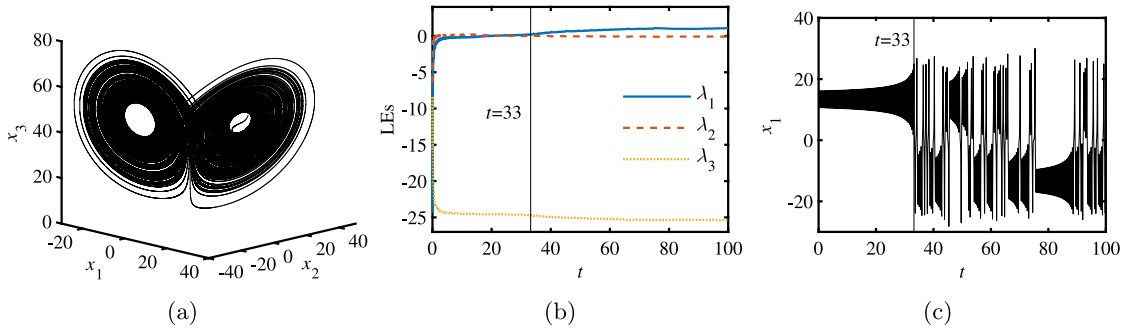

Fig. 1. The Q_1 test set of fractional-order Lorenz system. (a) Phase trajectory. (b) Time histories of LEs. (c) Time histories of x_1.

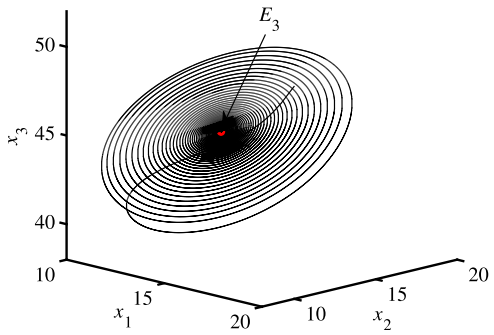

Fig. 2. Phase trajectory of fractional-order Lorenz system for the Q_2 test set.

Table 1
The correspondences [40] between the signs of LEs and the limit set of 4-D systems.

LEs	Limit set
$(+,+,0,-)$	Hyperchaos
$(+,0,-,-)$	Chaos
$(0,0,0,0)$	Quasi-period
$(0,-,-,-)$	Period

3.3. Nonautonomous case

Although only the autonomous system is discussed in the process of proposing the method, the proposed method can also be easily applied to nonautonomous systems by just rewriting them as the autonomous forms in the extended phase space. As the third example, the fractional-order Duffing oscillator [41,42] is demonstrated here, and it is governed by

$$\ddot{u} + c\dot{u} - u + u^3 + \beta D_t^p u = P_0 \cos \varphi t \tag{14}$$

In this case, the system parameters are taken as $c = 0.3$, $\beta = -0.1$, $P_0 = 0.255$, $\varphi = 1.2$, and the simulation conditions are set to $(u, \dot{u}, D_t^p u)|_{t=0} = (0,0,0)$, $h = 0.001$, $t_{\text{final}} = 300$, and $p \in (0,1]$. Then, the bifurcation and LEs are simulated, and the results are shown in Fig. 6(a) and 6(b), respectively. Note that the limit set of this forced oscillator cannot be the equilibrium point, hence there is always a LE that is 0, which is the characteristic of continuous-time systems [34]. To better reflect the dynamic behavior, the LLE here is the largest LE except 0, but not always the λ_1.

By comparing the LLE with bifurcation in Fig. 6, one can understand that the accuracy of LE determined by the proposed method is acceptable in a wide range of the order. Although there are small errors, it is not contrary to the methodology. As aforementioned, the integer-order case will be reduced to the forward Euler scheme, which has $O(h)$ accuracy. In fact, the accuracy of the discrete scheme Eqs. (4) based on G–L definition is also $O(h)$ (see Podlubny's proof [31]). One way to improve the accuracy of the proposed method is to apply the high-order numerical scheme. For recent numerical methods of FDEs, one can refer to Li, et al. [43] and Baleanu, et al. [44].

3.4. Comparison with previous methods

At the last, for comparison, the time series method [29] and the extended Benettin-Wolf algorithm [30] are applied to above three numerical examples. LEs of fractional-order Lorenz system calculated by such two methods and the proposed method are listed in Table 2. The results of Q_3 set in Table 2 show that the extended Benettin-Wolf algorithm is accurate in the standard integer-order case. However, for the Q_1 set, λ_1 calculated by the extended Benettin-Wolf algorithm is obviously different from other two methods. For the Q_2 set, λ_1 of both the extended Benettin-Wolf algorithm and the time series method are unreasonable, because the asymptotically stable equilibrium point means that all LEs must be negative. There is also a similar comparison result, as shown in Table 3, in which the LEs of the 4-D fractional-order Chen system calculated by the three different methods are listed. As suggested in Table 3, λ_1 determined by both the proposed method and the time series method is clearly different from the one obtained by the extended Benettin-Wolf algorithm, especially for the periodic motion, the result is not reasonable, since the sign of the corresponding LEs should be $(0,-,-,-)$. In addition, the extended Benettin-Wolf algorithm is also applied to calculate the LLE of fractional-order Duffing oscillator. As shown in Fig. 6(b), results obtained by the extended Benettin-Wolf algorithm are inconsistent with the bifurcation behavior in Fig. 6(a). In short, the proposed method works well in the above typical cases and it is superior to the two existing methods which are widely employed.

Above such discrepancies are mainly caused by the different descriptions for deviation. In the extended Benettin-Wolf algorithm, the deviation matrix is obtained from fractional-order variational equations, in which the different nonlocality caused by different derivative orders is ignored since all rows of the equations are simultaneously integrated. Therefore, the algorithm is more suitable for quasi-integer-order systems. In the time series method, the deviation is obtained by directly measuring the Euclidean distance between $\boldsymbol{x}(t)$ and $\overline{\boldsymbol{x}}(t)$. In this way, deviations cause by multiple initial perturbations is not orthogonalized. Thus, the deviation growth is always dominated by large Lyapunov exponents so that it is difficult to calculate all LEs. Also, if there is a LE close to another one, the result calculated by the time series method may be inaccurate, for example, the results of Q_2 test set in Table 2.

Moreover, it should be noted that the above discrepancies are not related to the use of different numerical schemes. Both the time series method and the extended Benettin-Wolf algorithm are supported by the Adams-type predictor–corrector numerical scheme [45,46]. In general, time histories simulated by different numerical schemes are quantitatively consistent for equilibrium point and (quasi) periodic

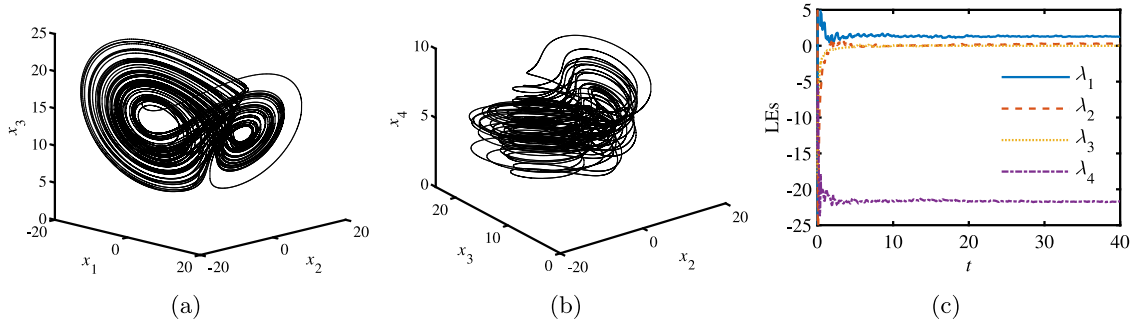

Fig. 3. Hyperchaotic attractor of 4-D fractional-order Chen system at $\alpha = 0.95$. (a) Phase trajectory in $x_1 - x_2 - x_3$ space. (b) Phase trajectory in $x_2 - x_3 - x_4$ space. (c) Time histories of LEs.

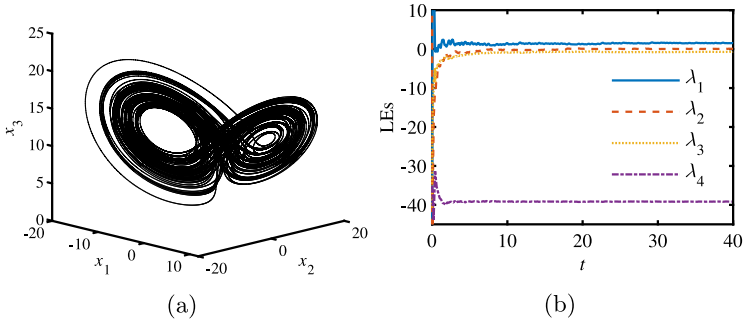

Fig. 4. Chaotic attractor of 4-D fractional-order Chen system at $\alpha = 0.88$. (a) Phase trajectory in $x_1 - x_2 - x_3$ space. (b) Time histories of LEs.

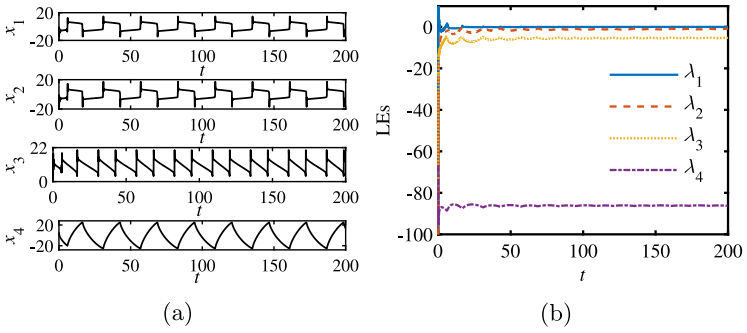

Fig. 5. Periodic motion of 4-D fractional-order Chen system at $\alpha = 0.78$. (a) Time histories of four state variables. (b) Time histories of LEs.

Table 2
LEs of fractional-order Lorenz system (12) simulated by the proposed method and other methods.

Test set	The proposed method	Time series method	Extended Benettin–Wolf algorithm	Limit set
Q_1	$\lambda_1 = 1.0586$ $\lambda_2 = -0.0933$ $\lambda_3 = -25.3930$	$\lambda_1 = 1.1540$	$\lambda_1 = 1.5994$ $\lambda_2 = 0.0020$ $\lambda_3 = -24.5707$	Chaos
Q_2	$\lambda_1 = -0.1391$ $\lambda_2 = -0.1581$ $\lambda_3 = -24.9487$	$\lambda_1 = 0.0144$	$\lambda_1 = 1.7311$ $\lambda_2 = -0.0041$ $\lambda_3 = -24.8305$	Asymptotically stable equilibrium point
Q_3	$\lambda_1 = 1.5143$ $\lambda_2 = 0.0617$ $\lambda_3 = -22.6085$	$\lambda_1 = 1.5520$	$\lambda_1 = 1.4921$ $\lambda_2 = -0.0037$ $\lambda_3 = -22.4878$	Chaos

response. Furthermore, chaotic responses simulated by different numerical schemes must be qualitatively consistent, since Tucker's theorem [47] ensures that the response of chaotic attractor relies on the genuine properties of the system itself rather than numerical method.

4. Conclusion

In conclusion, this paper is not the first work on LE of FOS, but indeed its nonlocality is pointed out, which is the reason why the well-established methods in integer-order systems are difficult to be

Table 3
LEs of the 4-D fractional-order Chen system (13) simulated by the proposed method and other methods.

The order	The proposed method	Time series method	Extended Benettin–Wolf algorithm	Limit set
$\alpha = 0.95$	$\lambda_1 = 1.2534$ $\lambda_2 = 0.2788$ $\lambda_3 = -0.0018$ $\lambda_4 = -21.6758$	$\lambda_1 = 1.0040$	$\lambda_1 = 2.1591$ $\lambda_2 = -0.0087$ $\lambda_3 = -0.0381$ $\lambda_4 = -16.2681$	Hyperchaos
$\alpha = 0.88$	$\lambda_1 = 1.5246$ $\lambda_2 = 0.0813$ $\lambda_3 = -0.6944$ $\lambda_4 = -39.1704$	$\lambda_1 = 1.2170$	$\lambda_1 = 2.7506$ $\lambda_2 = -0.0228$ $\lambda_3 = -0.0470$ $\lambda_4 = -22.7979$	Chaos
$\alpha = 0.78$	$\lambda_1 = 0.0066$ $\lambda_2 = -0.9901$ $\lambda_3 = -5.2612$ $\lambda_4 = -86.1648$	$\lambda_1 = 0.0482$	$\lambda_1 = 4.0483$ $\lambda_2 = 0.0244$ $\lambda_3 = -0.0145$ $\lambda_4 = -37.0781$	Period

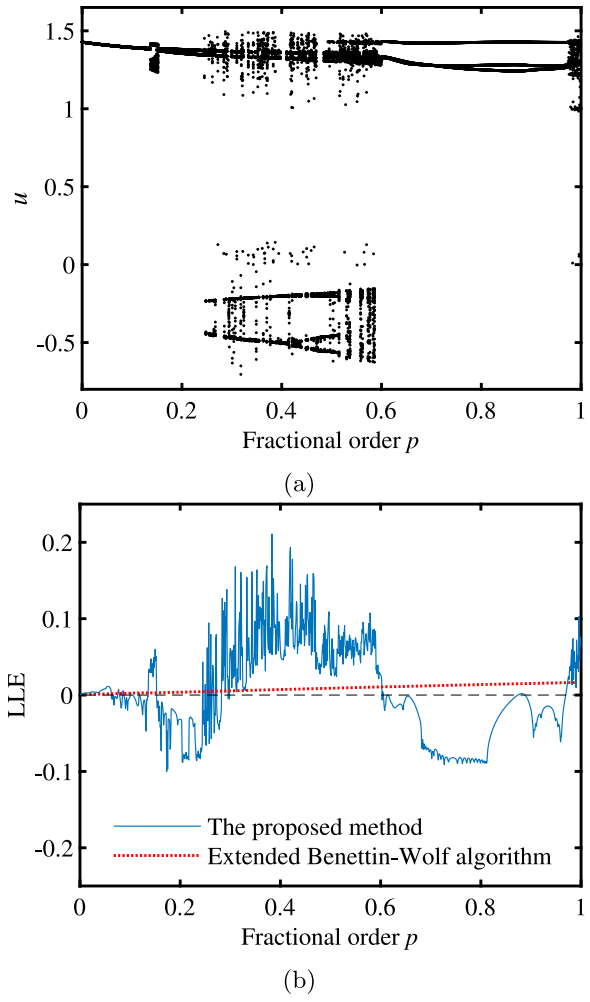

Fig. 6. Dynamic behavior of the fractional-order Duffing oscillator. (a) Bifurcation with p. (b) Evolution of the LLE with p.

generalized in FOS. Importantly, a general method for determining all LEs of FOS is proposed, and the methodological compatibility with the standard integer-order systems is naturally retained. The proposed method can be easily applied to the nonautonomous systems, and incommensurate systems without conversion to the commensurate form. As for systems with low effective order and hyperchaotic systems, the proposed method is also well applicable. In addition, the proposed method is superior to the previous methods in accuracy and correctness. All of these advantages have been verified by three classical fractional-order systems. In the future research, one can try to improve the accuracy based on other discretization methods.

CRediT authorship contribution statement

Hang Li: Conceptualization, Methodology, Formal analysis, Investigation, Writing – original draft. **Yongjun Shen:** Methodology, Funding acquisition, Resources, Supervision. **Yanjun Han:** Validation, Formal analysis. **Jinlu Dong:** Data curation, Writing – review & editing. **Jian Li:** Conceptualization, Funding acquisition, Supervision, Project administration.

Declaration of competing interest

The authors declare that they have no known competing financial interests or personal relationships that could have appeared to influence the work reported in this paper.

Data availability

All data that support the findings of this work are available from the corresponding author upon reasonable request.

Acknowledgments

This work is supported by the National Natural Science Foundation of China (Grant No. 12272091, No. 11172063, No. 11772206 and No. U1934201).

References

[1] Oseledets VI. A multiplicative ergodic theorem. Characteristic Ljapunov, exponents of dynamical systems. Trans Moscow Math Soc 1968;19:197–231.
[2] Benettin G, Galgani L, Giorgilli A, Strelcyn JM. Lyapunov characteristic exponents for smooth dynamical systems and for Hamiltonian systems; a method for computing all of them. Part 1: Theory. Meccanica 1980;15(1):9–20. http://dx.doi.org/10.1007/BF02128236.
[3] Wolf A, Swift JB, Swinney HL, Vastano JA. Determining Lyapunov exponents from a time series. Physica D 1985;16(3):285–317. http://dx.doi.org/10.1016/0167-2789(85)90011-9.
[4] Takens F. Detecting strange attractors in turbulence. Springer; 1981.
[5] Habib S, Ryne RD. Symplectic calculation of Lyapunov exponents. Phys Rev Lett 1995;74(1):70. http://dx.doi.org/10.1103/PhysRevLett.74.70.
[6] Lorenz EN. The local structure of a chaotic attractor in four dimensions. Physica D 1984;13(1–2):90–104. http://dx.doi.org/10.1016/0167-2789(84)90272-0.
[7] Bryant P, Brown R, Abarbanel HD. Lyapunov exponents from observed time series. Phys Rev Lett 1990;65(13):1523. http://dx.doi.org/10.1103/PhysRevLett.65.1523.
[8] Zeng X, Eykholt R, Pielke R. Estimating the Lyapunov-exponent spectrum from short time series of low precision. Phys Rev Lett 1991;66(25):3229. http://dx.doi.org/10.1103/PhysRevLett.66.3229.
[9] Balcerzak M, Dabrowski A, Blazejczyk-Okolewska B, Stefanski A. Determining Lyapunov exponents of non-smooth systems: Perturbation vectors approach. Mech Syst Signal Process 2020;141:106734. http://dx.doi.org/10.1016/j.ymssp.2020.106734.

[10] Soriano DC, Fazanaro FI, Suyama R, de Oliveira JR, Attux R, Madrid MK. A method for Lyapunov spectrum estimation using cloned dynamics and its application to the discontinuously-excited FitzHugh–Nagumo model. Nonlinear Dynam 2012;67(1):413–24. http://dx.doi.org/10.1007/s11071-011-9989-2.

[11] Stefanski A. Estimation of the largest Lyapunov exponent in systems with impacts. Chaos Solitons Fractals 2000;11(15):2443–51. http://dx.doi.org/10.1016/S0960-0779(00)00029-1.

[12] Wang G, Ding H, Chen L. Nonlinear normal modes and optimization of a square root nonlinear energy sink. Nonlinear Dynam 2021;104(2):1069–96. http://dx.doi.org/10.1007/s11071-021-06334-1.

[13] Vogl M, Rötzel PG. Chaoticity versus stochasticity in financial markets: Are daily S&P 500 return dynamics chaotic? Commun Nonlinear Sci Numer Simul 2022;108:106218. http://dx.doi.org/10.1016/j.cnsns.2021.106218.

[14] Zhou Y, Wang C, Liu C, Yong H, Zhang X. Optically triggered chaotic vortex avalanches in superconducting $YBa_2Cu_3O_{7-x}$ films. Phys Rev A 2020;13(2):024036. http://dx.doi.org/10.1103/PhysRevApplied.13.024036.

[15] Li H, Shen Y, Yang S, Peng M, Han Y. Simultaneous primary and super-harmonic resonance of Duffing oscillator. Acta Phys Sin 2021;70(4). http://dx.doi.org/10.7498/aps.70.20201059.

[16] Valério D, Machado JT, Kiryakova V. Some pioneers of the applications of fractional calculus. Fract Calc Appl Anal 2014;17(2):552–78. http://dx.doi.org/10.2478/s13540-014-0185-1.

[17] Sun L, Chen Y. Numerical analysis of variable fractional viscoelastic column based on two-dimensional Legendre wavelets algorithm. Chaos Solitons Fractals 2021;152:111372. http://dx.doi.org/10.1016/j.chaos.2021.111372.

[18] Meral F, Royston T, Magin R. Fractional calculus in viscoelasticity: an experimental study. Commun Nonlinear Sci Numer Simul 2010;15(4):939–45. http://dx.doi.org/10.1016/j.cnsns.2009.05.004.

[19] Hou J, Niu J, Shen Y, Yang S, Zhang W. Dynamic analysis and vibration control of two-degree-of-freedom boring bar with fractional-order model of magnetorheological fluid. J Vib Control 2022;28(21–22):3001–18. http://dx.doi.org/10.1177/10775463211023368.

[20] Kamal F, Elsonbaty A, Elsaid A. A novel fractional nonautonomous chaotic circuit model and its application to image encryption. Chaos Solitons Fractals 2021;144:110686. http://dx.doi.org/10.1016/j.chaos.2021.110686.

[21] Wang S, Hong L, Jiang J, Li X. Synchronization precision analysis of a fractional-order hyperchaos with application to image encryption. AIP Adv 2020;10(10):105316. http://dx.doi.org/10.1063/5.0012493.

[22] Naim M, Lahmidi F, Namir A, Kouidere A. Dynamics of an fractional SEIR epidemic model with infectivity in latent period and general nonlinear incidence rate. Chaos Solitons Fractals 2021;152:111456. http://dx.doi.org/10.1016/j.chaos.2021.111456.

[23] Higazy M. Novel fractional order SIDARTHE mathematical model of COVID-19 pandemic. Chaos Solitons Fractals 2020;138:110007. http://dx.doi.org/10.1016/j.chaos.2020.110007.

[24] Diethelm K, Kiryakova V, Luchko Y, Machado J, Tarasov VE. Trends, directions for further research, and some open problems of fractional calculus. Nonlinear Dynam 2022;107:3245–70. http://dx.doi.org/10.1007/s11071-021-07158-9.

[25] Sun H, Zhang Y, Baleanu D, Chen W, Chen Y. A new collection of real world applications of fractional calculus in science and engineering. Commun Nonlinear Sci Numer Simul 2018;64:213–31. http://dx.doi.org/10.1016/j.cnsns.2018.04.019.

[26] Li C, Ma Y. Fractional dynamical system and its linearization theorem. Nonlinear Dynam 2013;71(4):621–33. http://dx.doi.org/10.1007/s11071-012-0601-1.

[27] Li C, Gong Z, Qian D, Chen Y. On the bound of the Lyapunov exponents for the fractional differential systems. Chaos 2010;20(1):013127. http://dx.doi.org/10.1063/1.3314277.

[28] Grigorenko I, Grigorenko E. Chaotic dynamics of the fractional Lorenz system. Phys Rev Lett 2003;91(3):034101. http://dx.doi.org/10.1103/PhysRevLett.91.034101.

[29] Zhou S, Wang X. Simple estimation method for the largest Lyapunov exponent of continuous fractional-order differential equations. Phys A Stat Mech Appl 2021;563:125478. http://dx.doi.org/10.1016/j.physa.2020.125478.

[30] Danca MF. Matlab code for Lyapunov exponents of fractional-order systems, Part II: The noncommensurate case. Int J Bifurcation Chaos 2021;31(12):2150187. http://dx.doi.org/10.1142/S021812742150187X.

[31] Podlubny I. Fractional differential equations. Elsevier; 1998.

[32] Li C, Cai M. Theory and numerical approximations of fractional integrals and derivatives. Society for Industrial and Applied Mathematics (SIAM); 2019.

[33] Petráš I. Fractional-order nonlinear systems: modeling, analysis and simulation. Springer; 2011.

[34] Parker TS, Chua L. Practical numerical algorithms for chaotic systems. Springer; 2012.

[35] Wang S, Yu Y, Diao M. Hybrid projective synchronization of chaotic fractional order systems with different dimensions. Phys A Stat Mech Appl 2010;389(21):4981–8. http://dx.doi.org/10.1016/j.physa.2010.06.048.

[36] Zhang R, Yang S. Robust synchronization of two different fractional-order chaotic systems with unknown parameters using adaptive sliding mode approach. Nonlinear Dynam 2013;71(1):269–78. http://dx.doi.org/10.1007/s11071-012-0659-9.

[37] Cafagna D, Grassi G. Hyperchaos in the fractional-order Rössler system with lowest-order. Int J Bifurcation Chaos 2009;19(01):339–47. http://dx.doi.org/10.1142/S0218127409022890.

[38] Wu X, Lu H, Shen S. Synchronization of a new fractional-order hyperchaotic system. Phys Lett A 2009;373(27–28):2329–37. http://dx.doi.org/10.1016/j.physleta.2009.04.063.

[39] Hegazi A, Matouk A. Dynamical behaviors and synchronization in the fractional order hyperchaotic Chen system. Appl Math Lett 2011;24(11):1938–44. http://dx.doi.org/10.1016/j.aml.2011.05.025.

[40] Leng X, Gu S, Peng Q, Du B. Study on a four-dimensional fractional-order system with dissipative and conservative properties. Chaos Solitons Fractals 2021;150:111185. http://dx.doi.org/10.1016/j.chaos.2021.111185.

[41] Shen Y, Yang S, Xing H, Gao G. Primary resonance of Duffing oscillator with fractional-order derivative. Commun Nonlinear Sci Numer Simul 2012;17(7):3092–100. http://dx.doi.org/10.1016/j.cnsns.2011.11.024.

[42] Shen Y, Li H, Yang S, Peng M, Han Y. Primary and subharmonic simultaneous resonance of fractional-order duffing oscillator. Nonlinear Dynam 2020;102(3):1485–97. http://dx.doi.org/10.1007/s11071-020-06048-w.

[43] Li C, Zeng F. Numerical methods for fractional calculus. CRC Press; 2015.

[44] Baleanu D, Diethelm K, Scalas E, Trujillo JJ. Fractional calculus: models and numerical methods. World Scientific; 2012.

[45] Diethelm K, Ford NJ, Freed AD. A predictor-corrector approach for the numerical solution of fractional differential equations. Nonlinear Dynam 2002;29(1):3–22. http://dx.doi.org/10.1023/A:1016592219341.

[46] Garrappa R. Numerical solution of fractional differential equations: A survey and a software tutorial. Mathematics 2018;6(2):16. http://dx.doi.org/10.3390/math6020016.

[47] Tucker W. A rigorous ODE solver and Smale's 14th problem. Found Comput Math 2002;2(1):53–117. http://dx.doi.org/10.1007/s002080010018.